Lymphoma cell-driven IL-16 is expressed in activated B-cell-like diffuse large B-cell lymphomas and regulates the pro-tumor microenvironment

Xuwen Guan,[1,2,3,4*] Yi Wang,[1,2*] Teng Fang,[1,2] Jingya Wang,[5] Ru Li,[1,2] Mu Hao[1,2] and Lugui Qiu[1,2]

[1]State Key Laboratory of Experimental Hematology, National Clinical Research Center for Blood Diseases, Haihe Laboratory of Cell Ecosystem, Institute of Hematology and Blood Diseases Hospital, Chinese Academy of Medical Sciences and Peking Union Medical College; [2]Tianjin Institutes of Health Science; [3]Department of Hematology, Tianjin First Central Hospital; [4]Department of Hematology, Nankai University Affiliated First Central Hospital and [5]Tianjin Medical University Cancer Institute & Hospital, National Clinical Research Center for Cancer; Key Laboratory of Cancer Prevention and Therapy; Tianjin's Clinical Research Center for Cancer; Department of Thoracic Oncology, Tianjin Lung Cancer Center, Tianjin Cancer Institute & Hospital, Tianjin Medical University, Tianjin, PR China

XG and YW contributed equally as first authors.

Correspondence: L. Qiu
qiulg@ihcams.ac.cn

M. Hao
haomu@ihcams.ac.cn

Received: February 26, 2024.
Accepted: September 19, 2024.
Early view: September 26, 2024.

https://doi.org/10.3324/haematol.2024.285304

Abstract

The activated B-cell-like subtype of diffuse large B-cell lymphoma (ABC-DLBCL) displays a worse outcome than the germinal center B-cell-like subtype (GCB-DLBCL). Currently, targeting the tumor microenvironment (TME) is the most promising approach to cure DLBCL with profound molecular heterogeneity; however, the factors affecting the tumor-promoting TME of ABC-DLBCL remain elusive. Here, cytokine interleukin-16 (IL-16) is expressed in tumor cells of ABC-DLBCL and secreted by the cleavage of active caspase-3. The serum IL-16 levels are not only a sensitive marker of treatment response, but also positively correlated with unfavorable prognosis in DLBCL patients. While IL-16 shows few direct promotional effects on tumor cell growth *in vitro*, its bioactive form significantly promotes tumor progression *in vivo*. Mechanically, IL-16 increases the infiltration of macrophages by the chemotaxis of $CD4^+$ monocytes in the TME, enhancing angiogenesis and the expression of cytokine IL-6 and IL-10, as well as decreasing T-cell infiltration to accelerate tumor progression. This study demonstrates that IL-16 exerts a novel role in co-ordinating the bidirectional interactions between tumor progression and the TME. IMM0306, a fusion protein of CD20 mAb with the CD47 binding domain of SIRPα, reverses the tumor-promoting effects of IL-16, providing new insights into treatment strategy in ABC-DLBCL.

Introduction

Diffuse large B-cell lymphoma (DLBCL), which develops from mature B cells, represents the most common type of non-Hodgkin lymphoma. Currently, DLBCL is mainly classified as 2 distinct molecular subtypes based on cell-of-origin (COO): the germinal center B-cell-like subtype (GCB-DLBCL), and the activated B-cell-like subtype (ABC-DLBCL); 10-15% of cases are unclassifiable.[1] It has become increasingly evident that the elements of the tumor microenvironment (TME) favor cancer pathogenesis and progression, and the characteristics of the TME vary in different DLBCL subtypes.[2-4] For example, ABC-DLBCL had higher levels of macrophages than GCB-DLBCL,[5] and $CD163^+$ tumor-associated macrophages (M2-like) were associated with the poorest clinical outcome in ABC-DLBCL but not in GBC-DLBC.[3] Notably, ABC-DLBCL is associated with a worse prognosis and is more aggressive than GCB-DLBCL.[6] Therefore, distinct TME may confer different progression advantages on DLBCL.[3]

The integration of rituximab immunotherapy into CHOP chemotherapy for DLBCL treatment has markedly improved patient outcomes and cured over 60% of patients with DLBCL.[1,6,7] In addition, findings of pivotal clinical trials have presented anti-CD19 chimeric antigen receptor (CAR) T-cell therapy as a breakthrough in the treatment of relapsed or refractory (R/R) DLBCL.[8,9] The successes observed with both immunotherapies suggest, in part, that TME is a key target for the treatment of DLBCL. However, approximately 40% of patients remain insensitive to these existing treatments. Therefore, exploring the confounding factors that determine

the evolution of TME in the progression of DLBCL, especially the ABC subtype, may improve the management of DLBCL. Cytokines play an important role in linking tumor cells to the TME.[10] Recent studies have shown that cytokines contribute to the growth of ABC-DLBCL.[11-13] High-throughput RNA sequencing data show that IL-16 is higher in ABC-DLBCL than in GCB-DLBCL, as it is one of the transcripts belonging to multiple COO-related expression signatures which, indeed, distinguish ABC from GCB DLBCL.[14,15] The human IL-16 gene encodes a 631-amino acid precursor IL-16 (pre-IL-16) protein, and pre-IL-16 can be cleaved by active caspase-3 into C-terminal mature IL-16 via the cleavage sites (Asp510).[16] Mature IL-16 is generally characterized as a chemoattractant for $CD4^+$ immune cells, including T cells, mononuclear phagocytes (monocytes, macrophages, and dendritic cells), and mast cells.[17-23] Studies showed that IL-16 is expressed and released by B cells and other immune cells (such as T cells, eosinophils, and dendritic cells).[17,24-26] However, its role in many B-cell malignancies, especially in DLBCL, has not yet been sufficiently studied.[27,28]

In this study, we aimed to investigate the distinct pattern of IL-16 expression in the normal lymph node and DLBCL, and specifically to explore its contribution to the bidirectional interactions between tumor progression. Our findings demonstrated that the IL-16, a non-canonical cytokine highly expressed in ABC-DLBCL, was cleaved and secreted by active caspase-3. Serum IL-16 levels could be used as a sensitive marker of treatment response and poor prognosis in DLBCL. In addition, the bioactive-driven IL-16 strengthened the progression of DLBCL through regulating macrophage enrichment, which provided new insights into the personalized treatment strategy for ABC-DLBCL.

Methods

Reagents or resources

All the key reagents or resources used in the study are to be found in *Online Supplementary Table S1*.

Mice models

Six-week-old female BALB/c nude mice (absence of thymus, absence of T cells), BALB/c mice (immunocompetent), and NOD SCID mice (T- and B-lymphocyte dysfunction, low natural killer [NK] cell and complement binding capacity) (Beijing Vital River Laboratory Animal Technology Co. Ltd.) were used in this study. Mice were randomly assigned to treatment groups before the start of each experiment. The investigators were not blinded during the collection or analysis of data.

Study approval

Serum samples were obtained from 87 DLBCL patients and 10 healthy donors. Peripheral blood was obtained from healthy donors. Clinical information on DLBCL patients has been provided in *Online Supplementary Table S2*. Biopsy specimens were obtained from 2 DLBCL patients. Written informed consent was obtained from all participants, and this study was approved by the ethics committee of the Institute of Hematology & Blood Diseases Hospital, Tianjin, China (approval number KT2020031-ER-2).

Commercial tissue microarrays (TMA) with 15 tonsil tissue and 70 DLBCL tissue samples were purchased from Shanghai Outdo Biotech Company Co. Ltd. (HLymB085PT01, Shanghai, China). Furthermore, this study was approved by the ethics committee of Shanghai Outdo Biotech Company Co. Ltd. (approval number SHYJS-CP-1910014).

For animal studies, ethical approval was obtained from the Ethics Committee of the Institute of Hematology & Blood Diseases Hospital, Tianjin, China (approval number KT2020031-ER-2).

For mice models, cell line culture, public databases and bioinformatics, plasmid construction, virus production, and transduction, IHC, IHF, mIHC etc., see the *Online Supplementary Methods*.

Results

IL-16 expression in lymph node B cells

IL-16 is abundant in immune cells.[17,24-26] Initially, we examined the expression and distribution of IL-16 in human tonsillar lymph nodes (N=15) by multi-immunofluorescence staining (mIHC) and found that $IL\text{-}16^+$ cells were mainly distributed in $CD20^+$ B cells (*Online Supplementary Figure S1A, B*). We next assessed the expression and distribution of IL-16 in B cell-enriched germinal centers. The result showed that most of the B cells located in the mantle zone expressed IL-16, and a few B cells located in the light and dark zone expressed IL-16, suggesting that IL-16 is differentially expressed in different types of B cells (Figure 1A, B). We then confirmed this by performing conventional IHC (*Online Supplementary Figure S1C*). Furthermore, we found IL-16 was highly abundant in naïve B cells (NB), memory B cells (MB), and plasma cells (PC) (non-light/dark areas), and relatively low in germinal center centroblasts (CB) and centrocytes (CC) (light/dark areas) (Figure 1C). Because BCL-6 is a key transcriptional repressor that regulates germinal center B-cell differentiation and may repress the expression of IL-16 in germinal center B cells,[29] we analyzed the expression of BCL-6. In an inverse trend to IL-16, BCL-6 expression was perfectly observed in CB and CC but not in NB, MB, or PC (Figure 1D). These findings showed that IL-16 was expressed differentially in mature B cells, and its expression in B cells could be regulated by BCL-6.

IL-16 is highly expressed in activated B-cell-like subtype of diffuse large B-cell lymphoma or non-germinal center B-cell-like subtype

Diffuse large B-cell lymphoma originates from mature B cells

at different stages of differentiation.[1] The GCB-DLBCL originates from centrocytes, whereas the ABC-DLBCL originates from PC or MB.[30] The gene expression data of 1,663 DLBCL patients (693 ABC-DLBCL and 970 GCB-DLBCL) from GEO databases were analyzed. The gene expression between the GCB-DLBCL and ABC-DLBCL groups was compared; 360 differential expression genes (DEG) were found. Pathway enrichment analysis showed that the cytokine-cytokine receptor interaction pathway was significantly enriched in the DEG, and IL-16 was highly expressed in ABC-DLBCL (Figure 2A, *Online Supplementary Figure S2A*).

We further confirmed whether IL-16 is differentially expressed in DLBCL in 2 authoritative databases with more DLBCL typing.[31,32] In particular, the highest level of IL-16 expression was found in the ABC subtype, followed by the unclassified-DLBCL, and the lowest expression was found in the GCB subtype. Moreover, IL-16 expression was higher in N1/MCD or C1/C5 (mainly ABC-DLBCL) and lower in BN2/EZB or C4/C3 (mainly GCB-DLBCL). We performed mIHC on DLBCL specimens (N=70) for further validation (Figure 2D). IL-16 was predominantly expressed in DLBCL tissues in tumor cells, and non-GCB-DLBCL (ABC- and unclassified-DLBCL) had a higher proportion of IL-16$^+$ cells compared to GCB-DLBCL (Figure 2E-H). We then confirmed this by performing conventional IHC (*Online Supplementary Figure S2B, C*). Collectively, IL-16 was highly expressed in ABC-DLBCL or non-GCB-DLBCL.

Serum IL-16 is secreted at high levels in activated B-cell-like subtype of diffuse large B-cell lymphoma

Next, we investigated the level of IL-16 in the serum of DLCBL patients (N=84) and healthy donors (N=10) by ELISA. Serum IL-16 levels were elevated in ABC-DLBCL, while there were no significant differences between healthy donors and GCB-DLBCL (Figure 3A, *Online Supplementary Figure S3A*). We then investigated the relationship between IL-16 levels in DLBCL and clinical prognosis, and found that high IL-16 secretion was associated with poor prognosis (overall survival [OS] / progression-free survival [PFS]) (Figure 3B). Consistent with previous studies, patients with ABC-DLBCL had a worse clinical prognosis compared to GCB-DLBCL patients (OS/PFS) (*Online Supplementary Figure S3B*). To exclude interference, we verified the relationship between IL-16 levels and clinical prognosis in patients with ABC-DBCL and showed that IL-16 levels were also associated with poor prognosis (OS/PFS) (Figure 3C). In addition, IL-16 levels were correlated with the International Prognostic Index and treatment response (*Online Supplementary Figure S3C, D*). Moreover, IL-16 levels were positively correlated with LDH and β_2M, suggesting an association between IL-16 and tumor burden (Figure 2D). We then explored whether IL-16 levels varied with changes in tumor burden after treatment, and found that *de novo* ABC-DLBCL patients with reduced tumor burden (complete response [CR] and partial response [PR]) had decreased IL-

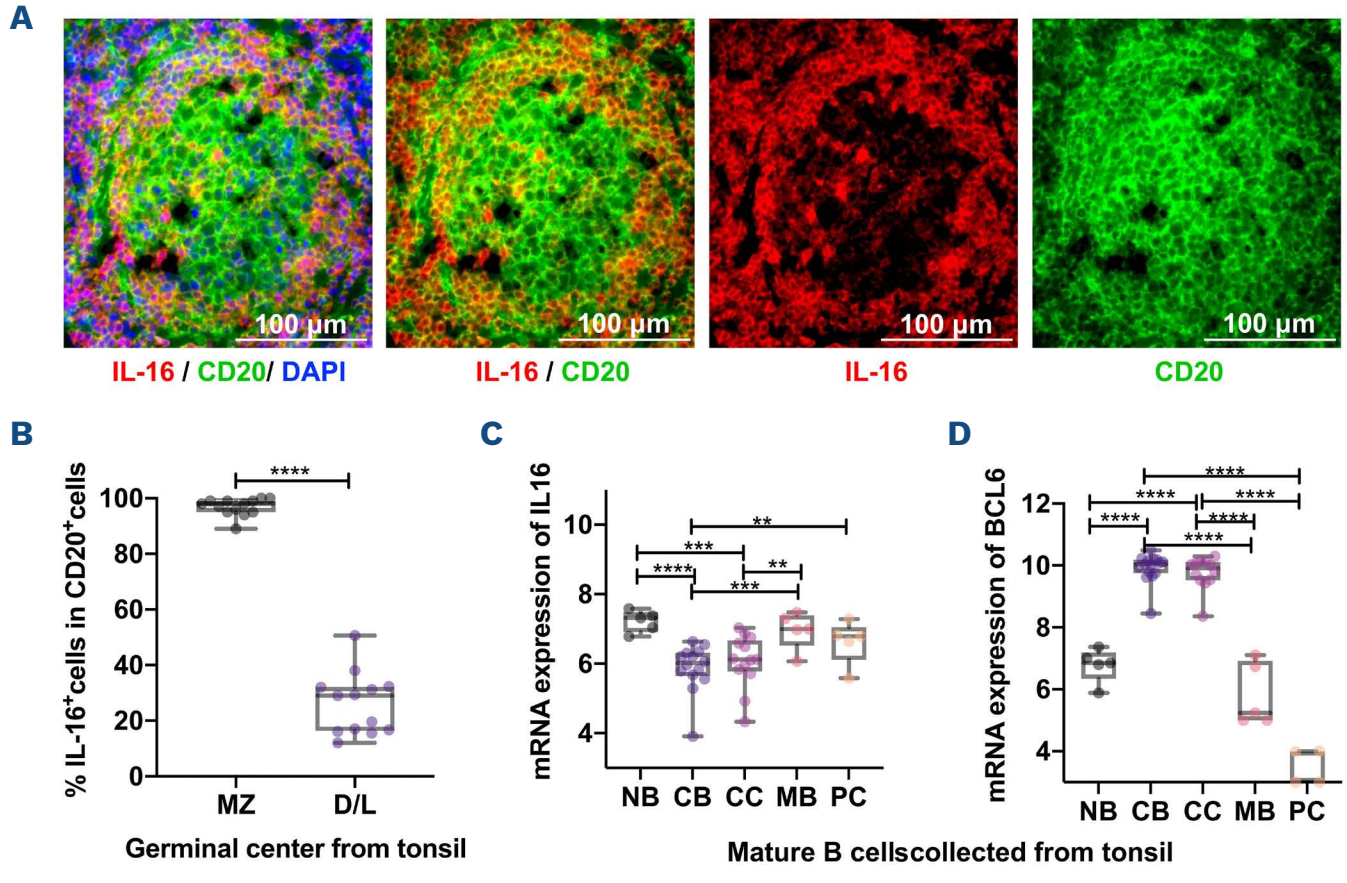

Figure 1. IL-16 expression in lymph node B cells. (A) Representative multi-immunofluorescence staining (mIHC) images for IL-16 protein expression (red pseudocolor) in the germinal center from tonsil specimens. CD20 (B cells, green pseudocolor) and DAPI nuclear stain (blue pseudocolor) included to discern tissue landscape. Scale bars apply across each row. (B) Proportion of IL-16-positive cells in different types of B cells, N=15. (C and D) Expression of IL-16 and BCL-6 mRNA in mature B cells from tonsil at different stages of differentiation. Naïve B cells (NB) (N=5), germinal center centroblasts (CB) (N=14), centrocytes (CC) (N=13), memory B cells (MB) (N=5), plasma cells (PC) (N=5). Gene expression data were collected from GEO, GSE2350. Data shown are mean ± Standard Deviation. *P* values are based on unpaired *t* test. ns: non-significant, ***P*<0.01, ****P*<0.001, *****P*<0.0001. D/L: dark/light zone; MZ: mantle zone.

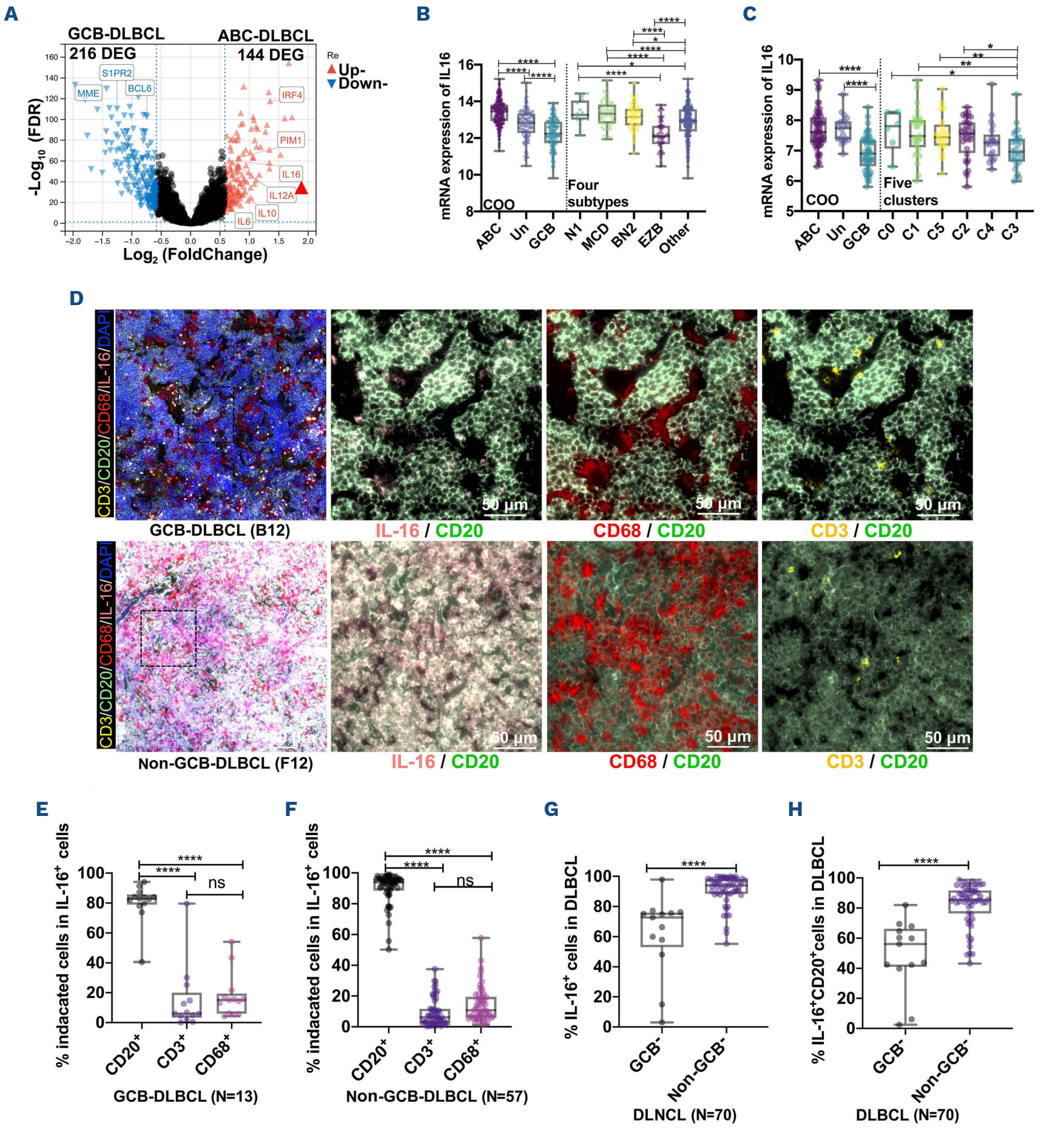

Figure 2. IL-16 is highly expressed in the activated B-cell-like subtype or the non-germinal center B-cell-like subtype of diffuse large B-cell lymphoma. (A) Volcano map indicates the differentially expressed genes (DEG) between germinal center B-cell-like subtype diffuse large B-cell lymphoma (GCB-DLBCL) (N=970) and activated B-cell-like subtype of DLBCL (ABC-DLBCL) (N=693) from 4 merged DLBCL databases (GSE10846, GSE31312, GSE87371, and GSE117556) (Fold Change [FC] >1.5, False Discovery Rate [FDR] <0.05). Red triangle indicates IL-16 highly expressed in ABC-DLBCL. (B) Difference in IL-16 mRNA expression between different types of DLBCL (gene expression data from Schimitz *et al.*[31]). (C) Difference in IL-16 mRNA expression between different types of DLBCL (gene expression data from Chapuy *et al.*[32]). (D) Representative multi-immunofluorescence staining images for IL-16 protein expression (pink pseudocolor) in non-GCB-DLBCL and GCB-DLBCL specimens. CD20 (tumor cells, green pseudocolor), CD3 (T cells, yellow pseudocolor), CD68 (macrophages, red pseudocolor), and DAPI nuclear stain (blue pseudocolor) included to discern tissue landscape. Scale bars apply across each row. (E) Proportion of IL-16-positive cells in the GCB-DLBCL (N=13) or (F) non-GCB-DLBCL (N=57) tumor cells ($CD20^+$) and different types of immune cells ($CD3^+$ T cells and $CD68^+$ macrophages). (G) Proportion of IL-16-positive cells or (H) IL-16-CD20 double positive cells in the DLBCL (N=70) specimens. Data shown are mean ± Standard Deviation. *P* values are based on unpaired *t* test. ns: non-significant, **P*<0.05, ***P*<0.01, *****P*<0.0001.

16-levels after being treated with R-CHOP-like treatment, but this was not the case in patients with stable disease (SD) and progressive disease (PD) (Figure 3E). Similarly, in patients with R/R ABC-DLBCL treated with CD19 CAR T-cell therapy, IL-16 decreased when tumor burden decreased, and increased when the tumor progressed (Figure 3F). To further identify the cytokines in ABC-DLBCL that correlated with the change in tumor burden, an inflammation antibody array was used to determine the levels of cytokines in sequential serum samples collected from a patient with ABC-DLBCL. We observed that IL-16, IL-3, IL-13, IFN-γ, and MIG were significantly down-regulated during disease remission. In contrast, during disease progression, an opposite trend was observed, indicating the existence of a positive correlation between these cytokines and tumor burden in ABC-DLBCL (*Online Supplementary Figure S3E*). These findings indicate that IL-16 levels are high in the serum of ABC-DLBCL patients, and IL-16 levels could be used to indicate treatment response and clinical prognosis.

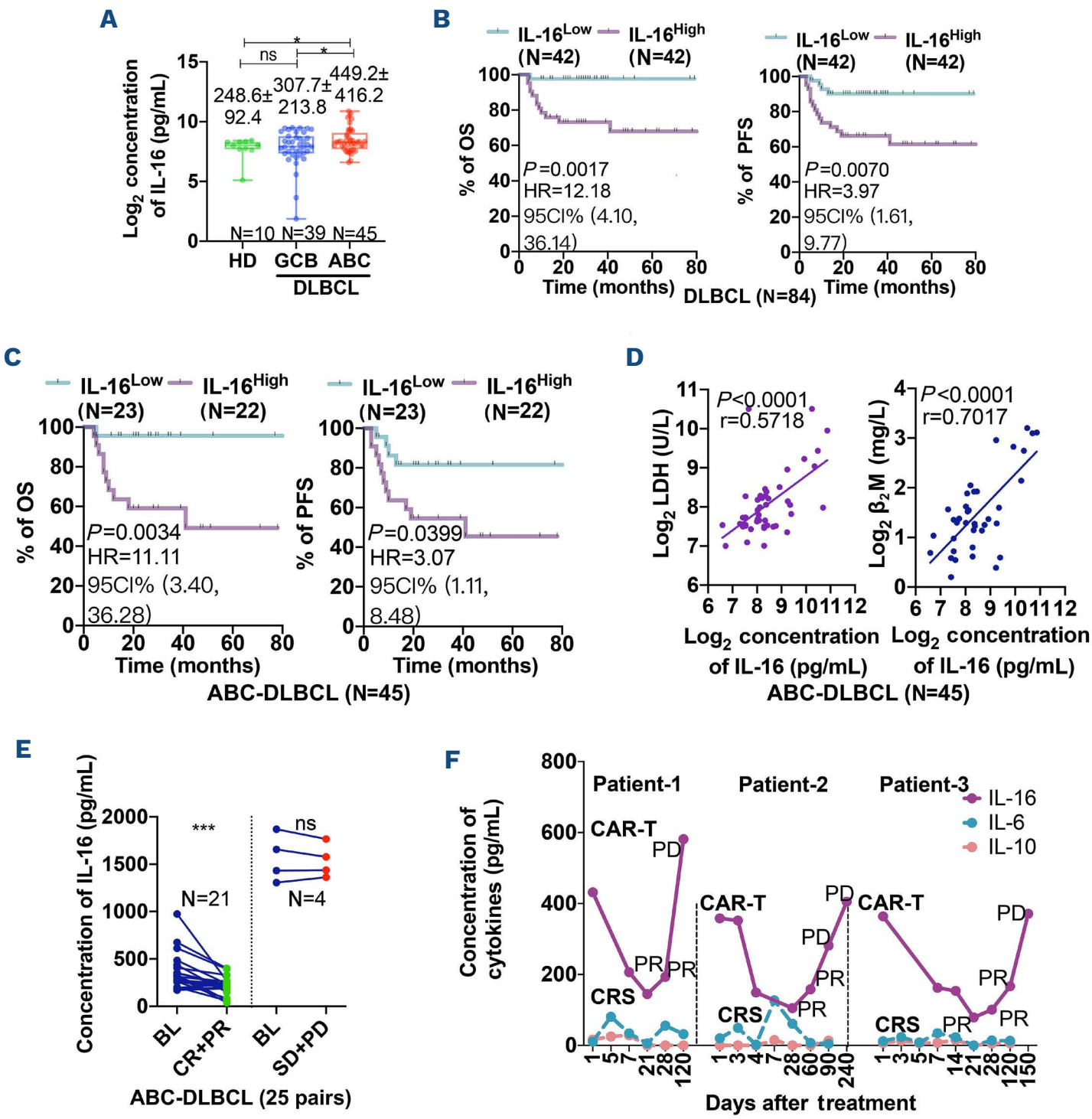

Figure 3. Serum IL-16 is secreted at high levels in activated B-cell-like subtype of diffuse large B-cell lymphoma. (A) Detection of serum IL-16 levels from 39 germinal center B-cell-like subtype of diffuse large B-cell lymphoma (GCB-DLBCL) patients, 45 activated B-cell-like subtype of DLBCL (ABC-DLBCL) patients, and 10 healthy donors by ELISA. (B) Overall survival (OS) and (C) progression-free survival (PFS) of DLBCL patients or ABC-DLBCL patients based on low and high levels of serum IL-16. (D) Correlations between serum IL-16 of ABC-DLBCL patients and lactate dehydrogenase (LDH) or β_2M are analyzed, N=45. (E) Detection of serum IL-16 levels from 25 pairs of *de novo* DLBCL patients (before treatment and after at least 2 cycles of treatment) by ELISA. Differences in IL-16 between the 2 time points are analyzed. (Left) Patients who achieved complete response (CR) and partial response (PR) after treatment (N=21). (Right) Patients achieving stable disease (SD) or with progressive disease (PD) after treatment (N=4). BL: patients' pre-treatment baseline serum levels. (F) Dynamic changes in serum IL-16, IL-6, and IL-10 in 3 relapsed refractory (R/R) ABC-DLBCL patients during anti-CD19 CAR T-cell (CAR-T) therapy at indicated time points. CRS: patients with cytokine release syndrome. Data shown are mean ± Standard Deviation. *P* values are based on unpaired or paired *t* test, log rank (Mantel-Cox) test, and Pearson correlation. ns: non-significant, **P*<0.05, ****P*<0.001.

Caspase-3 regulates IL-16 cleavage and secretion in diffuse large B-cell lymphoma

Recent studies indicate that full-length IL-16 (80kDa, pre-IL-16) is not secreted intracellularly and its secretion depends on the cleavage of activated caspase-3 into 20kDa mature IL-16. We then assessed the underlying regulatory mechanism of IL-16 secretion in DLBCL. These results revealed that, consistent with previous findings, mRNA and protein expression of IL-16 was elevated in the ABC-DLBCL cell line and decreased in GCB-DLBCL. However, IL-16 at 20kDa was

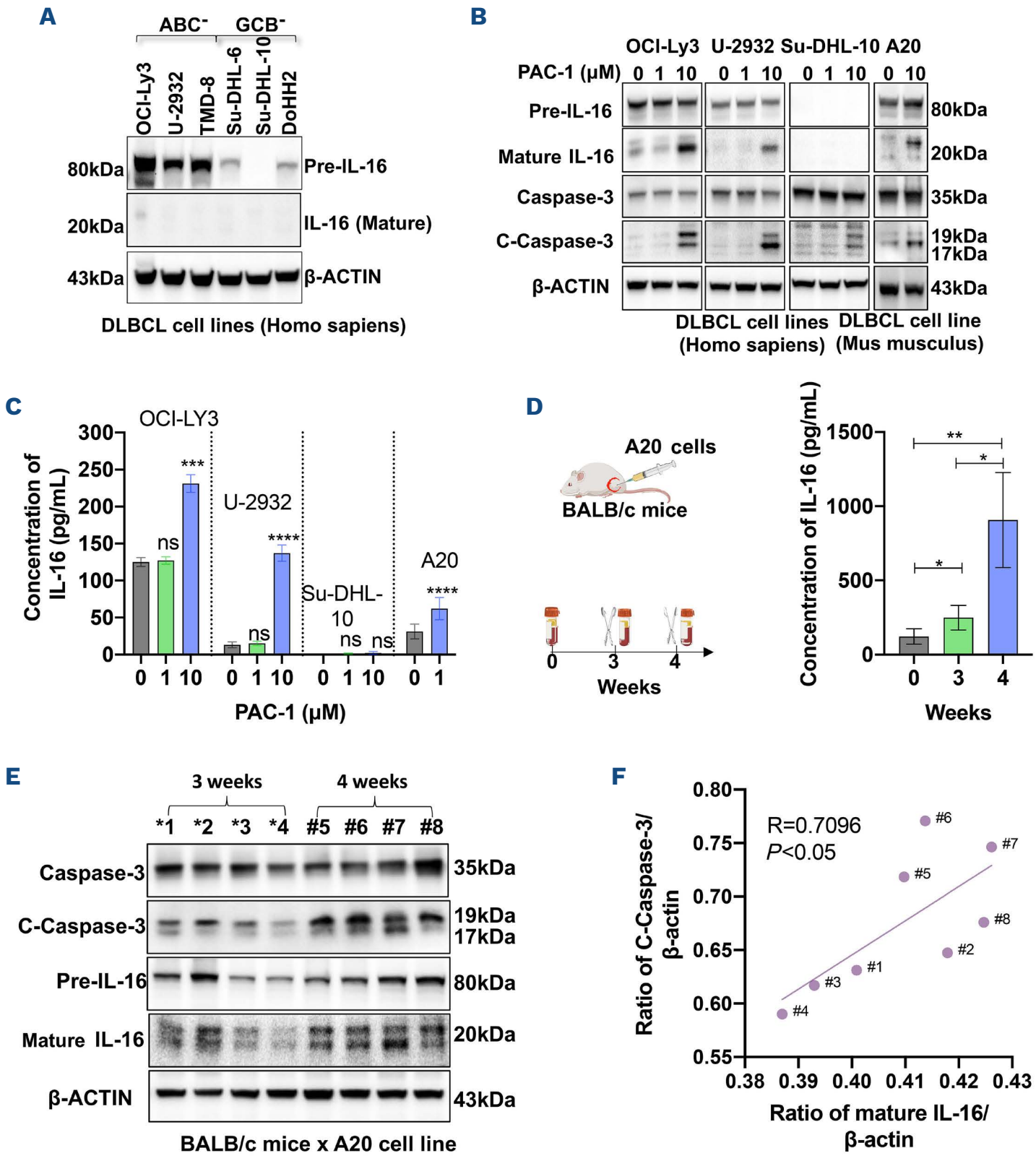

Figure 4. Caspase-3 regulates IL-16 cleavage and secretion in diffuse large B-cell lymphoma. (A) Detection of IL-16 protein expression in diffuse large B-cell lymphoma (DLBCL) cell lines (activated B-cell-like subtype of DLBCL [ABC-DLBCL] cell lines: OCI-Ly3, U-2932, and TMD-8; germinal center B-cell-like subtype of DLBCL [GCB-DLBCL] cell lines: Su-DHL-6, Su-DHL-10, and DoHH2) by Western blotting. β-actin is used as a loading control. 80kDa IL-16 indicates full-length Pre-IL-16, and 20kDa IL-16 indicates cleaved mature IL-16. (B and C) Human DLBCL cell lines (OCI-Ly3, U-2932, and Su-DHL-10) and murine DLBCL cell lines (A20) are treated with indicated dose of PAC-1 for 24 hours, and (B) protein expression of IL-16 and Caspase-3 are determined by Western blotting. β-actin is used as a loading control. C-Caspase-3 indicated cleaved Caspase-3. (C) Secretion levels of IL-16 in the culture medium are quantified by ELISA. (D-F) BALB/c mice were inoculated subcutaneously with A20 cells (N=4/group). Serum was collected at different time points (week 0, week 3 and week 4), and the tumor tissues were collected at different time points (week 3 and week 4). (D) Detection of mice serum IL-16 levels. (E) Detection of IL-16 and Caspase-3 protein expression by Western blotting in different DLBCL tissues. β-actin is used as loading control. (F) Correlation between C-Caspase-3 and mature IL-16 expression. Data shown are mean ± Standard Deviation. *P* values are based on unpaired *t* test and Pearson correlation. ns: non-significant, **P*<0.05, ***P*<0.01, ****P*<0.001, *****P*<0.0001.

expressed at a low level in the DLBCL cell lines (Figure 4A, *Online Supplementary Figure S4A*). In addition, we found that DLBCL cell lines secreted less IL-16 when untreated, suggesting that IL-16 in DLBCL secretes low levels of IL-16 *in vitro* (*Online Supplementary Figure S4B*).

To further understand whether caspase-3 is orchestrating the activation and secretion of IL-16 in DLBCL, the caspase-3 activator PAC-1 was utilized to promote the activation of caspase-3. It was revealed that PAC-1 enhanced the expression of IL-16 at 20kDa, whereas no expression of IL-16 at 20kDa was observed for the IL-16-negative Su-DHL-10-cell line despite increased caspase-3 activation. Similarly, PAC-1 stimulated caspase-3 activation and 20kDa IL-16 expression in murine DLBCL cell line A20. Subsequently, we also found that PAC-1 contributed to IL-16 secretion (Figure 4B, C). A dose of PAC-1 (10 μM) capable of inducing IL-16 secretion promoted apoptosis in less than 20% of ABC-DLBCL cells (*Online Supplementary Figure S4C*). Therefore, caspase-3 is critical for promoting IL-16 activation and secretion in DLBCL, and the reason for the low IL-16 secretion *in vitro* is that caspase-3 is barely activated in these conditions (*Online Supplementary Figure S2D*).

We then investigated the *in vivo* role of IL-16 activation and secretion in BALB/c mice through subcutaneous injection of murine DLBCL cell line A20 (Figure 4D). Tumor volume and IL-16 secretion were positively correlated, with 20kDa IL-16 and activated caspase-3 being expressed in tumor tissue and having higher expression in larger tumors (3 weeks *vs.* 4 weeks) (Figure 4D, E, O*nline Supplementary Figure S4E*). Notably, 20kDa IL-16 and activated caspase-3 were positively correlated (Figure 4F). Thus, *in vivo*, tumor tissues expressed activated caspase-3 and 20kDa IL-16, and secreted IL-16. These results underline that IL-16 secretion in DLBCL is regulated by caspase-3 and is tumor-tissue-dependent.

IL-16 promotes tumor growth *in vivo*

To the best of our knowledge, there are no relevant studies on the effect of IL-16 on DLBCL tumor cells. To do this, we generated lentivirus infection with stable overexpression of IL-16$^{\Delta 511\text{-}631aa}$ (labeled with IL-16$^{\Delta}$) or EV in ABC-DLBCL cell lines (U-2932 and TMD-8), and verified its overexpression by Western blotting and ELISA (Figure 5A). Cell proliferation was detected by CCK8 assay, and essentially no effect was found on the growth of the tumor cells themselves *in vitro* (*Online Supplementary Figure S5*). Overexpression of IL-16$^{\Delta 511\text{-}631aa}$ also did not affect the cell cycle, the apoptosis in these cells, or the response of these cells to vincristine, doxorubicin, and 4-OOH-CY *in vitro* (*Online Supplementary Figure S5B-D*). Similarly, recombinant human IL-16 (rh-IL-16) had no significant effect on the proliferation of primary cells from DLBCL tissues and DLBCL cell lines (*Online Supplementary Figure S5E*). Stable downexpression of pre-IL-16 (80kDa) in ABC-DLBCL cell lines (U-2932 and TMD-8) also did not affect cell growth, cell cycle, or apoptosis in these cells, or the response of these cells to the tested drugs *in vitro* (*Online Supplementary Figure S6A-E*). Furthermore, bulk RNA-seq data showed that pre-IL-16 downexpression had minimal effect on the gene expression in ABC-DLBCL cell lines (U-2932 and TMD-8) (*Online Supplementary Figure S6F*). Moreover, stable overexpression of pre-IL-16 (80kDa) also had no significant effect on cell growth *in vitro* (*Online Supplementary Figure S6G, H*). Studies have shown that IL-16 can directly promote the growth of myeloma cells with the help of CD4 or CD9 receptors.[28] However, the expression of CD4 or CD9 on the cell surface of ABC-DLBCL cells (OCI-Ly3, U-2932, and TMD-8) was low, but the expression of CD9 on the cell surface of myeloma cells (RPMI-8226) was high (*Online Supplementary Figure S6 I*).

Unexpectedly, *in vivo* NOD SCID mice (T-cell deficiency) inoculated with stable overexpression of IL-16$^{\Delta 511\text{-}631aa}$ U-2932 cells exhibited apparent promotion of tumor growth (Figure 5B, C). The same experiments were validated with murine DLBCL cell line A20. We generated lentivirus infection with stable overexpression of murine IL-16$^{\Delta 507\text{-}624aa}$ (labeled with IL-16$^{\Delta}$) or EV in A20 cell lines, and verified its overexpression by Western blotting and ELISA (Figure 5D). It was found that IL-16 at 20kDa did not affect the growth of tumor cells *in vitro* (*Online Supplementary Figure S7A*), but significantly promoted tumor growth in both immunodeficient BALB/c nude mice (T-cell deficiency) (*Online Supplementary Figure S7B-D*) and immunocompetent BALB/C mice (Figure 5E, F). It is suggested that IL-16 has no marked tumor-promoting effect on tumor cells themselves, but may contribute to tumor growth indirectly through other potential mechanisms.

IL-16 promotes tumor growth dependent on macrophages *in vivo*

In order to understand how IL-16 is orchestrating the changes within the tumor microenvironments and inflammation of immune cells (such as dendritic cells, plasmacytoid, neutrophils, NK cells, T cells, and macrophages), we performed immunostaining in the immunodeficient BALB/c nude mice with A20-tumor-burden between different groups (murine IL-16$^{\Delta 507\text{-}624aa}$ overexpression *vs.* EV) (*Online Supplementary Figure S8A, B*). The marker of macrophages F4/80 displayed a notable increase in the overexpression group (*Online Supplementary Figure S8A*). Similar results could be expected in human-derived U-2932 cells induced in NOD SCID mice (*Online Supplementary Figure S8C*) and murine-derived A20 cells induced in BALB/c mice (Figure 6A). In addition, our mIHC results in DLBCL specimens (N=70) showed that there was a significant positive correlation between the proportion of IL-16^{+}CD20^{+} cells in tumor cells and the proportion of CD68^{+} macrophages in non-tumor cells (Figure 2D, *Online Supplementary Figure S8D)*. These results show that IL-16 promotes macrophage infiltration.

When the A20-tumor-burden BALB/c nude mice were treated with the macrophage scavenger clodronate liposomes or control (Saline), the tumor-promoting effect of IL-16 was obviously reduced after removal of mouse macrophages

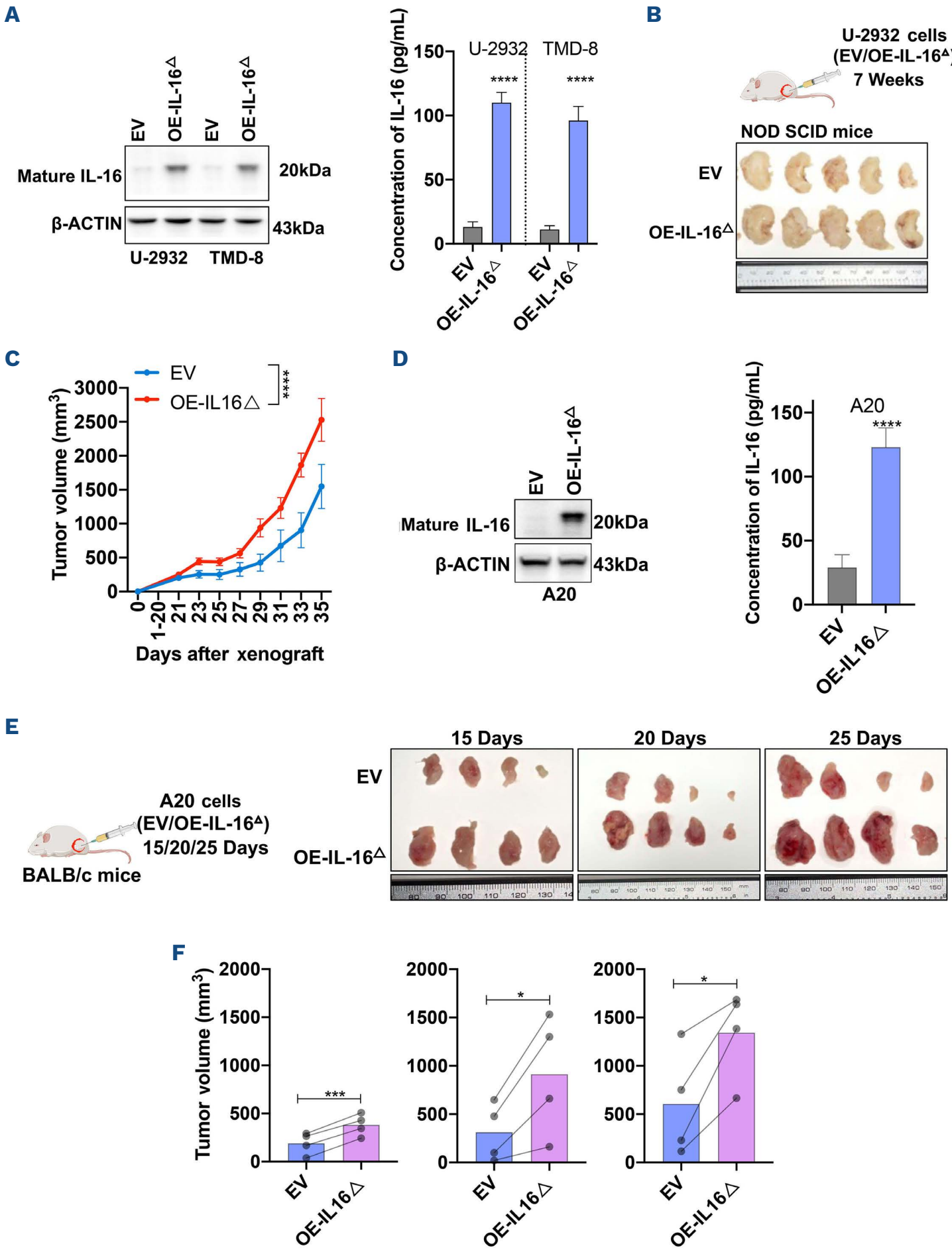

Figure 5. IL-16 promotes tumor growth *in vivo*. (A) Detection of IL-16 protein expression by Western blotting in diffuse large B-cell lymphoma (DLBCL) cell lines (U-2932 and TMD-8) with stable overexpression of IL-16$^{\Delta 511\text{-}631aa}$ (labeled with IL-16$^{\Delta}$) or EV. β-actin is used as a loading control. IL-16 secretion levels in the culture medium of indicated DLBCL cell lines (U-2932 and TMD-8 with stable overexpression of IL-16$^{\Delta 511\text{-}631aa}$ (labeled with IL-16$^{\Delta}$) or empty vector controls (EV) (5x10^5 cells/mL, 24 hours [hr]) are quantified by ELISA. (B and C) NOD SCID mice are inoculated with U-2932 cells with overexpression of IL-16$^{\Delta 511\text{-}631aa}$ (labeled with IL-16$^{\Delta}$) or EV respectively (N=5/group). Comparison of volumes of tumors growing subcutaneously in mice. When tumors are palpable, tumor volumes are measured and calculated every other day. When the mice were anesthetized and sacrificed, the tumor samples were collected to measure volume. (D) Detection of mature IL-16 protein expression by Western blotting in A20 cells with stable murine IL-16$^{\Delta 507\text{-}624aa}$ overexpression or EV. β-actin is used as a loading control. Secretion levels of IL-16 in the culture medium of A20 cell lines with stable overexpression of murine IL-16$^{\Delta 507\text{-}624aa}$ or EV (5x10^5 cells/mL, 24 hr) are quantified by ELISA. (E and F) BALB/c mice are inoculated with A20 cells with murine IL-16$^{\Delta 507\text{-}624aa}$ overexpression or EV, respectively, for 15/20/25 days (N=4/group). Collection of tumors and tumor volumes from mice. Data shown are mean ± Standard Deviation. *P* values are based on two-way ANOVA and unpaired or paired *t* test. ns: non-significant, *P<0.05, ***P<0.001, ****P<0.0001.

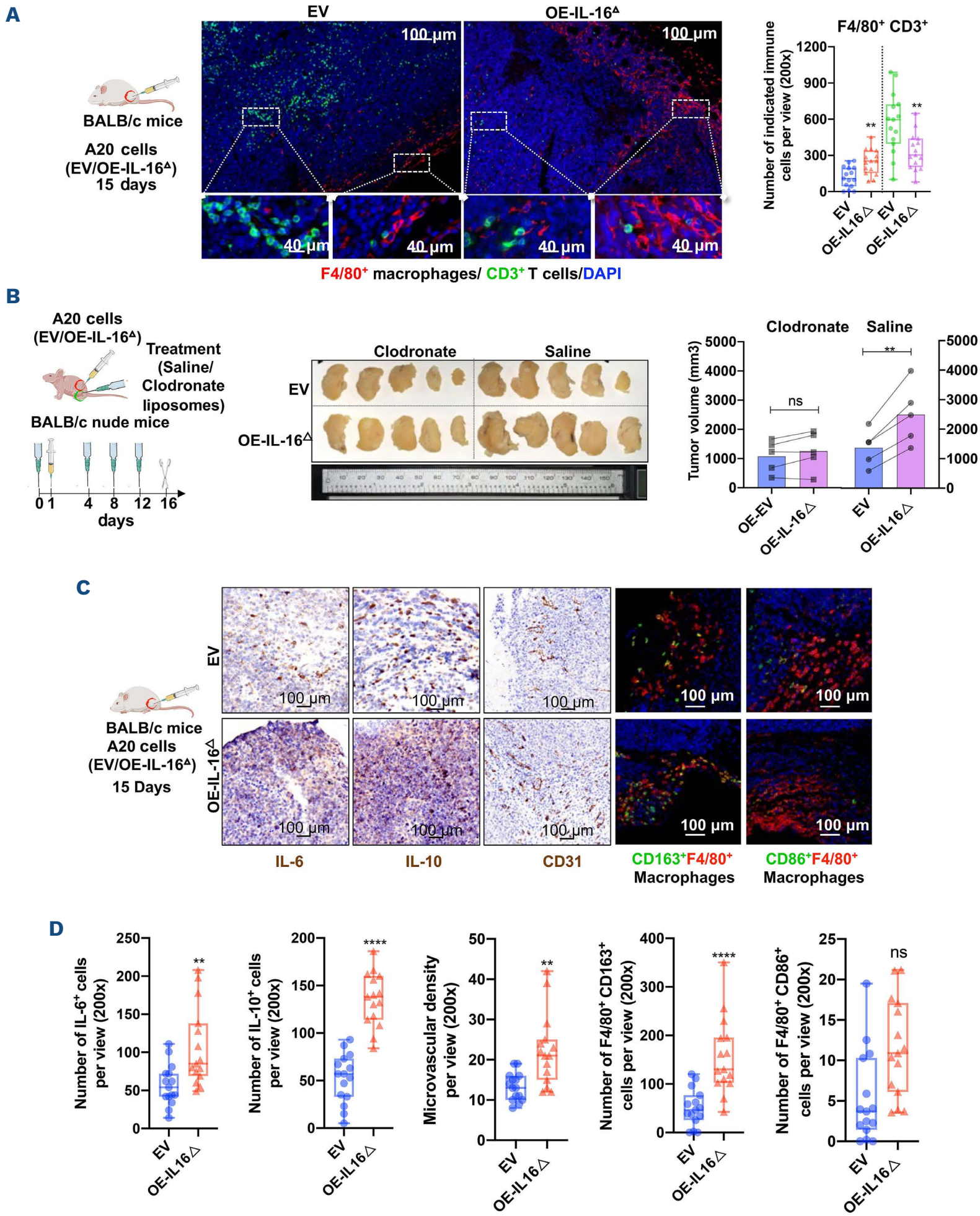

Figure 6. IL-16 promotes tumor growth dependent on macrophages *in vivo*. (A) Representative immunostaining and quantification for T-cell markers CD3 and macrophage marker F4/80 in the sections of tumor tissues from BALB/c mice. Difference in infiltration of indicated cells in tumor tissues between different groups (murine IL-16$^{\Delta 507\text{-}624aa}$ overexpression *vs.* empty vector controls [EV]) is analyzed. Scale bars apply across each row. (B) BALB/c nude mice are inoculated with A20 cells with murine IL-16$^{\Delta 507\text{-}624aa}$ overexpression or EV, respectively (N=5/group) on Day 1. Mice are treated with Control (saline) or Clodronate liposomes at indicated time points (Days 0, 4, 8, 12, intraperitoneal [i.p.]). When the mice were anesthetized and sacrificed, the tumor samples were collected to measure volume. (C and D) Representative immunostaining and quantification for the cytokines IL-6 and IL-10, vascular endothelial cells marker CD31 (microvascular density), CD163 and F4/80, and CD86 and F4/80, in the sections of tumor tissues from BALB/c mice. Difference in infiltration of indicated cells in tumor tissues between different groups (murine IL-16$^{\Delta 507\text{-}624aa}$ overexpression *vs.* EV) is analyzed. Scale bars apply across each row. Data shown are mean ± Standard Deviation. *P* values are based on unpaired or paired *t* test. ns: non-significant, ***P*<0.01, *****P*<0.0001.

(Figure 6B). Reportedly, macrophages promote tumor development primarily by enhancing angiogenesis as well as the expression and secretion of cytokines, such as IL-6 (directly promoting tumor growth) and IL-10 (exerting immunosuppressive effects). Representative immunostaining for the cytokines IL-6 and IL-10, as well as angiogenesis biomarker CD31 in the sections of tumor tissues from either A20 cell line-induced BALB/c nude mice or A20 cell line-induced BALB/c mice, suggesting IL-16 markedly enhanced the expression of IL-6, IL-10, and angiogenesis in the macrophage compartment regardless of immunodeficiency (Figure 6C, D, *Online Supplementary Figure S9A*). We then examined the polarized form of macrophages in A20 cell line-induced BALB/c mice, and showed that macrophages tended to be M2 polarized and there were more M2 macrophages in the IL-16 overexpression group (Figure 6C, D). Lastly, but notably, representative staining for H&E and mIHC of T-cell markers CD3, CD8, CD4, FOXP3, and T-Bet in the sections of tumor biopsy from A20 cell line-induced BALB/c mice suggested IL-16 inhibited infiltration of anti-tumor T cells in immunocompetent mice (Figure 6A, *Online Supplementary Figure S9B-D*). Overall, these results suggest that IL-16 facilitates macrophage infiltration, mainly of M2 macrophages, to promote tumor growth.

Migration of CD4$^+$ monocytes induced by diffuse large B-cell lymphoma-derived IL-16

Macrophages in the TME are mainly derived from peripheral blood monocytes, which is regulated by chemokines. IL-16 mediates chemotaxis mainly through the CD4 receptor. To verify chemotaxis of DLBCL-derived IL-16 on different types of immune cells, we collected the culture medium (CM) of these DLBCL cells (U-2932 and TMD-8 cells with stable overexpression of IL-16$^{\triangle 511\text{-}631aa}$ or EV) and determined the cell migration of peripheral blood leukocytes (PBL). IL-16 did not essentially affect the overall chemotaxis of leukocytes (*Online Supplementary Figure S10A*). We then analyzed the composition of migrated leukocytes induced by the indicated CM by flow cytometry and found that IL-16 did not statistically affect leukocyte composition (*Online Supplementary Figure S10B*). We then revealed that IL-16 promoted chemotaxis of monocytes but did not affect chemotaxis of various types of T cells (*Online Supplementary Figure S10C, D*). Since only a relatively low proportion of leukocytes are monocytes, we isolated monocytes and found they were divided into 2 categories: CD11b$^+$CD14^{++} monocytes with CD4$^+$, and CD11b$^+$CD14$^+$ monocytes with CD4$^-$ (Figure 7A). Results showed that IL-16 notably increased monocyte chemotaxis, mainly CD11b$^+$CD14^{++} monocytes with CD4$^+$

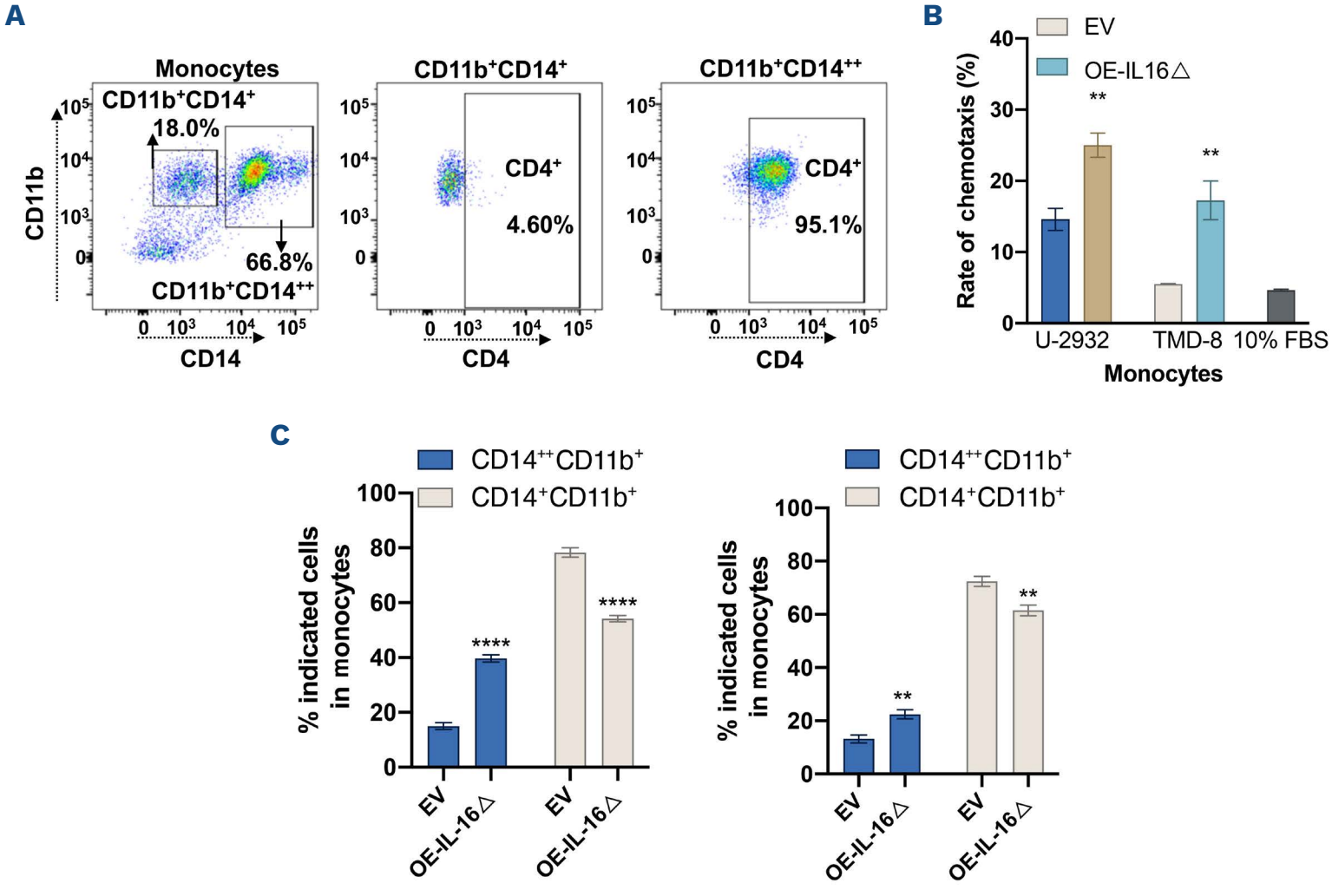

Figure 7. The migration of CD4$^+$ monocytes induced by diffuse large B-cell lymphoma-derived IL-16. (A) Monocytes were isolated from healthy donors and were stained with anti-CD11b-APC-Cy7, anti-CD14-APC, anti-CD4-FITC antibodies. (B) Cell migration of monocytes is determined by transwell assay (1 hour) combined with the CCK-8 test. 10% FBS culture medium were used as control. Rate of chemotaxis (%)=($OD_{Lower\ chamber}$-$OD_{Background}$/ $OD_{Upper\ chamber}$-$OD_{Background}$)x100. (C) the proportion of indicated monocytes in migrated monocytes. Data shown are mean ± Standard Deviation. *P* values are based on unpaired *t* test. ns: non-significant, ***P*<0.01, *****P*<0.0001.

(Figure 7B, C). These results suggest that DLBCL-derived IL-16 significantly promotes $CD4^+$ monocyte chemotaxis, by which it promotes macrophage infiltration.

IMM0306 effectively inhibits the growth of diffuse large B-cell lymphoma with high IL-16 expression

Studies showed that anti-CD47 blockade limited tumor growth in lymphoma with increased tumor-associated macrophages.[33] Multiple therapeutic antibodies, such as rituximab and antibodies targeting CD47, target tumor cells for macrophage clearance by antibody-dependent cellular phagocytosis (ADCP),[33,34] and the macrophage : tumor ratio determined the effect of ADCP.[20]

IMM0306, a novel fusion protein of CD20 mAb with the CD47 binding domain of SIRPα, exerts excellent cancer killing efficacy by activating macrophages via blockade of CD47-SIRPα interaction and FcγR engagement by simultaneously binding to CD47 and CD20 of B cells.[35] We then examined whether IMM0306 could reverse the pro-tumorigenic effects of IL-16 in ABC-DLBCL.

Given that IL-16 promoted macrophage infiltration in DLBCL, we first confirmed whether increasing the macrophage : tumor ratio would enhance IMM0306-induced ADCP. The ABC-DLBCL cells were co-cultured with effector cells with different ratios as indicated, and then we treated the mixed cells with IMM0306 or IgG1 mAb control. IMM0306 significantly promoted ADCP and increased the effector cell : tumor cell ratio, further increasing the efficacy of IMM0306 (Figure 8A). Next, IMM0306 was used to treat ABC-DLBCL *in vivo*. Pre-IL-16 was over-expressed in the U2932 cell line via lentivirus infection (*Online Supplementary Figure S6G*) and NOD SCID mice were subcutaneously inoculated with the indicated tumor cells. Mice were treated with IMM0306 and placebo, respectively. Consistently, pre-IL-16 significantly promoted tumor growth in the placebo group. However, IMM0306 had a better therapeutic effect in the pre-IL-16 overexpression group than in the placebo group (Figure 8B-D). This preliminary preclinical study suggests that IMM0306 has promising antitumor effects in ABC-DLBCL with high IL-16 expression.

Discussion

In this study, we found that IL-16 was differentially expressed in different mature B cells. IL-16 was seen to be expressed in the tumor cells of ABC-DLBCL. The serum of ABC-DLBCL patients had elevated IL-16, which could predict the clinical prognosis and response to treatment. IL-16 secretion was tumor-tissue-dependent, which could promote tumor growth through increasing macrophage enrichment in the TME. Lastly, IL-16 specifically induced the $CD4^+$ monocyte chemotaxis that promotes macrophage infiltration. IMM0306, which exerts cancer killing efficacy by activating macrophages, was a novel treatment approach in ABC-DLBCL.

Most DLBCL can be classified into 2 distinct molecular subtypes based on COO.[1] Notably, ABC-DLBCL is more aggressive and associated with a worse prognosis than GCB-DLBCL.[6] The new classifications based on transcriptional and mutational signatures, somatic copy number alterations, and structural variants have distinguished up to 4 distinct subtypes (MCD, BN2, N1, and EZB) or 5 clusters (known as C1-C5).[31,32] In this study, IL-16 was found to be highly expressed in ABC-DLBCL or ABC-DLBCL-enriched N1/MCD or C1/C5 subtypes. Studies demonstrated that ABC-DLBCL develops from GC B cells undergoing plasmablast or memory cell differentiation, while GCB-DLBCL develops from GC light zone B cells.[30,36-38] In addition, our study showed that IL-16 was more abundant in plasma cells and memory cells but not GC light zone B cells, suggesting that different levels of IL-16 expression in DLBCL may be attributed to it being a differentiation factor for B cells.

Currently, the metabolic tumor volume (MTV) calculated by FDG-PET/CT parameters and circulating tumor DNA (ctDNA) are relatively reliable strategies to assess the tumor burden and therapeutic response in DLBCL patients.[39,40] In this study, we found IL-16 was detectable in the serum of patients with ABC-DLBCL, and as a non-invasive biomarker, serum IL-16 levels can function as effective adverse prognostic factors. We observed that a dynamic change in serum IL-16 levels could predict treatment response in patients with DLBCL who receive R-CHOP or anti-CD19 CAR T-cell therapy. Next, we will also compare its accuracy and usefulness with MTV and ctDNA in the ABC-DLBCL patients.

IL-16 is not a typical cytokine that is directly secreted from cells, the secretion of which depends on active caspase-3.[16,41] In this study, IL-16 secretion in DLBCL was regulated by caspase-3 which was tumor-tissue-dependent. Few previous studies have explored the role and mechanisms of IL-16 in DLBCL. In this study, we found IL-16 did not affect DLBCL cell growth *in vitro*, but its secretion accelerates tumor growth in both immunodeficient and immunologically-competent mouse models. Mechanically, IL-16 was found to increase the infiltration of macrophages and triggered angiogenesis, IL-6 and IL-10 expression, and decreased the infiltration of T cells in tumor tissues.[42] Macrophage clearance could reduce the tumor-promoting effect of IL-16. Moreover, DLBCL derived IL-16 significantly promotes $CD4^+$ monocyte chemotaxis, by which it promotes macrophage infiltration. Two recent pivotal studies distinguish 4 subtypes of the DLBCL microenvironment (GC-like, mesenchymal, inflammatory, and depleted), or 9 lymphoma ecotypes (LE1-LE9) based on the transcriptional footprint of microenvironment cells or single-cell RNA-sequencing (scRNA-seq). Macrophages were abundant in inflammatory, LE1, LE4 subtypes which contain a higher proportion of ABC-DLBC.[3,43] It has been demonstrated that ABC-DLBCL had higher levels of macrophages than GCB-DLBCL,[5] and infiltration of macrophages in the TME is associated with poor prognosis and correlates with chemotherapy resistance in most cancers.[44] Our study

suggests that IL-16 is a key factor regulating the tumor microenvironment in ABC-DLBCL.

Tumor-associated macrophages facilitate tumor progression in most cancers; therefore, therapies targeting macrophages have been a topic of recent studies.[44] The macrophage-dependent ADCP is the principal cytotoxic mechanism for rituximab,[34] and the proportion of macrophages determined the effect of ADCP.[20] In this study, we hypothesized that

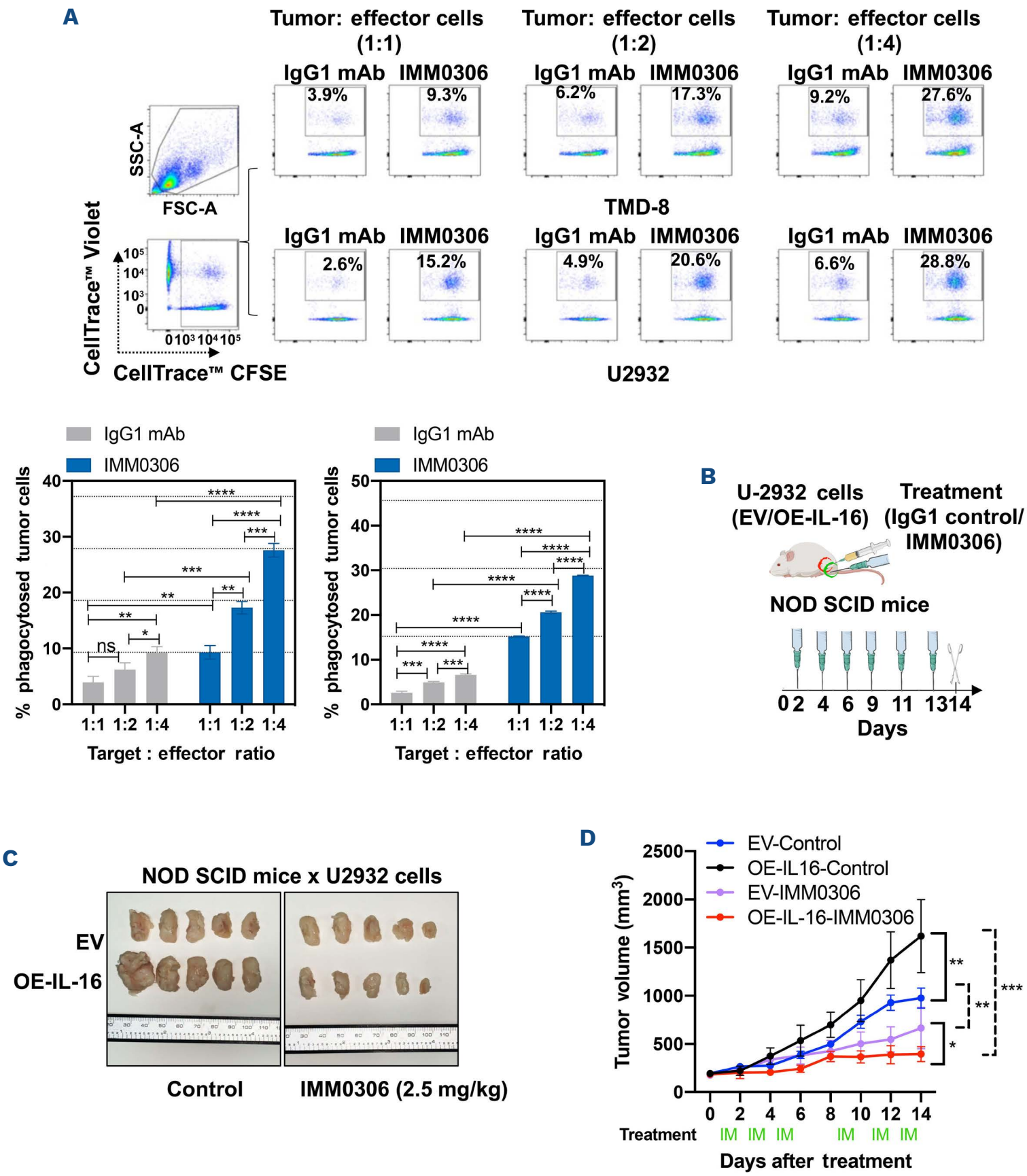

Figure 8. Antitumor effects of IMM0306 in activated B-cell-like subtype of diffuse large B-cell lymphoma. (A) Diffuse large B-cell lymphoma (DLBCL) cells (TMD-8 and U-2932) are labeled with CellTrace™ CFSE, and effector cells (THP-1, a human macrophage / monocyte cell line) are labeled with CellTrace™ Violet. Tumor cells are co-cultured with effector cells at the indicated ratio for 30 minutes with the 10 μg/mL IMM0306 or IgG1 mAb treatment. CellTrace™ CFSE$^+$ tumor cells are selected to analyze the percentage of CellTrace™ CFSE$^+$ CellTrace™ Violet$^+$ tumor cells phagocytosed by effector cells (ADCP). (B-D) NOD SCID mice are inoculated with U-2932 cells with pre-IL-16 overexpression or empty vector Controls (EV), respectively (N=5/group). When the tumors reached a mean of 200 mm^3, mice were treated with Control (placebo : human IgG1 control, 2.5 mg/kg, intravenous [i.v.], Days 2, 4, 6, 9, 11, and 13) and IMM0306 (2.5 mg/kg, i.v., Days 2, 4, 6, 9, 11, and 13). Volumes of tumors of mice were measured and calculated every other day after treatment. Data shown are mean ± Standard Deviation. *P* values are based on the two-way ANOVA and the unpaired or paired *t* test. ns: non-significant, **P*<0.05, ***P*<0.01, ****P*<0.001, *****P*<0.0001.

activating IL-16-recruited macrophages might reverse its pro-tumorigenic effects. IMM0306 is a novel fusion protein of CD20 mAb with the CD47 binding domain of SIRPα and exerts cancer killing efficacy by activating macrophages.[35] In this study, IMM0306 had an excellent therapeutic effect in ABC-DLBCL with high IL-16 expression. Both in the pre-clinical study and in a pivotal clinical trial, the combinations of anti-CD47 antibody and anti-CD20 antibody augmented the macrophage-dependent ADCP effect in DLBCL, particularly in ABC-DLBCL.[45,46] A clinical trial is being designed to evaluate the potential for clinical applications of IMM0306 in ABC-DLBCL.

In conclusion, our study shows that IL-16 promote tumor growth by co-ordinating the cross-communications between the lymphoma cells and TME *in vivo*, which further suggests that IL-16 is responsible for the progression of ABC-DLBCL as a source of non-oncogene addiction and is responsible for the progression of ABC-DLBCL. Therefore, targeting the pro-tumor mechanisms of IL-16 could provide an attractive biology-driven personalized treatment strategy to deal with therapeutic vulnerability in ABC-DLBCL.

Disclosures

No conflicts of interest to disclose.

Contributions

XG conceived and designed the project, performed experiments, analyzed data, and wrote the paper. YW was responsible for animal management, ELISA, and collected clinical data of patients. JW performed the IHF and IHC. RL cultured the cell lines. TF, LQ and MH analyzed the results and critically revised the manuscript. All authors provided critical review and revisions, and approved the final version of the manuscript for publication.

Acknowledgments

We are grateful to the healthy volunteers for participation in our study. We are also grateful to ImmuneOnco Biotech (Shanghai, China) who supported IMM0306.

Funding

This investigation was supported by CAMS Innovation Fund for Medical Sciences (CIFMS) (2023-I2M-2-007) (to LQ), National Natural Science Foundation of China (82341211) (to LQ), National Natural Science Foundation of China (82170194, 82370210) (to MH), National Natural Science Foundation of China (82000208) (to XG), National Natural Science Foundation of China (82203628) (to JW), and Tianjin Health Research Project (TJWJ2023QN027) (to XG).

Data-sharing statement

The data that support the findings of this study are available from the corresponding author upon reasonable request.

References

1. Sehn LH, Salles G. Diffuse large B-cell lymphoma. N Engl J Med. 2021;384(9):842-858.
2. Scott DW, Gascoyne RD. The tumour microenvironment in B cell lymphomas. Nat Rev Cancer. 2014;14(8):517-534.
3. Kotlov N, Bagaev A, Revuelta MV, et al. Clinical and biological subtypes of B-cell lymphoma revealed by microenvironmental signatures. Cancer Discov. 2021;1(6):1468-1489.
4. Riihijarvi S, Fiskvik I, Taskinen M, et al. Prognostic influence of macrophages in patients with diffuse large B-cell lymphoma: a correlative study from a Nordic phase II trial. Haematologica. 2015;100(2):238-245.
5. Xu-Monette ZY, Xiao M, Au Q, et al. Immune profiling and quantitative analysis decipher the clinical role of immune-checkpoint expression in the tumor immune microenvironment of DLBCL. Cancer Immunol Res. 2019;7(4):644-657.
6. Bakhshi TJ, Georgel PT. Genetic and epigenetic determinants of diffuse large B-cell lymphoma. Blood Cancer J. 2020;10(12):123.
7. Flowers CR, Sinha R, Vose JM. Improving outcomes for patients with diffuse large B-cell lymphoma. CA Cancer J Clin. 2010;60(6):393-408.
8. Abramson JS, Palomba ML, Gordon LI, et al. Lisocabtagene maraleucel for patients with relapsed or refractory large B-cell lymphomas (TRANSCEND NHL 001): a multicentre seamless design study. Lancet. 2020;396(10254):839-852.
9. Neelapu SS, Locke FL, Bartlett NL, et al. Axicabtagene ciloleucel CAR T-cell therapy in refractory large B-cell lymphoma. N Engl J Med. 2017;377(26):2531-2544.
10. Galdiero MR, Marone G, Mantovani A. Cancer inflammation and cytokines. Cold Spring Harb Perspect Biol. 2018;10(8):a028662.
11. Hashwah H, Bertram K, Stirm K, et al. The IL-6 signaling complex is a critical driver, negative prognostic factor, and therapeutic target in diffuse large B-cell lymphoma. EMBO Mol Med. 2019;11(10):e10576.
12. Gupta M, Han JJ, Stenson M, et al. Elevated serum IL-10 levels in diffuse large B-cell lymphoma: a mechanism of aberrant JAK2 activation. Blood. 2012;119(12):2844-2853.
13. Beguelin W, Sawh S, Chambwe N, et al. IL10 receptor is a novel therapeutic target in DLBCLs. Leukemia. 2015;29(8):1684-1694.
14. Reddy A, Zhang J, Davis NS, et al. Genetic and functional drivers of diffuse large B cell lymphoma. Cell. 2017;171(2):481-494.e15.
15. Wright G, Tan B, Rosenwald A, Hurt EH, Wiestner A, Staudt LM. A gene expression-based method to diagnose clinically distinct subgroups of diffuse large B cell lymphoma. Proc Natl Acad Sci U S A. 2003;100(17):9991-9996.
16. Richmond J, Tuzova M, Cruikshank W, Center D. Regulation of cellular processes by interleukin-16 in homeostasis and cancer. J Cell Physiol. 2014;229(2):139-147.
17. Kaser A, Dunzendorfer S, Offner FA, et al. B lymphocyte-derived IL-16 attracts dendritic cells and Th cells. J Immunol. 2000;165(5):2474-2480.
18. Lynch EA, Heijens CA, Horst NF, Center DM, Cruikshank WW. Cutting edge: IL-16/CD4 preferentially induces Th1 cell migration: requirement of CCR5. J Immunol. 2003;171(10):4965-4968.
19. McFadden C, Morgan R, Rahangdale S, et al. Preferential

migration of T regulatory cells induced by IL-16. J Immunol. 2007;179(10):6439-6445.
20. Lossos C, Liu Y, Kolb KE, et al. Mechanisms of lymphoma clearance induced by high-dose alkylating agents. Cancer Discov. 2019;9(7):944-961.
21. Bernstein HB, Plasterer MC, Schiff SE, Kitchen CM, Kitchen S, Zack JA. CD4 expression on activated NK cells: ligation of CD4 induces cytokine expression and cell migration. J Immunol. 2006;177(6):3669-3676.
22. Cruikshank W, Little F. lnterleukin-16: the ins and outs of regulating T-cell activation. Crit Rev Immunol. 2008;28(6):467-483.
23. Qi JC, Wang J, Mandadi S, et al. Human and mouse mast cells use the tetraspanin CD9 as an alternate interleukin-16 receptor. Blood. 2006;107(1):135-142.
24. Liu S, Lei Z, Li J, et al. Interleukin 16 contributes to gammaherpesvirus pathogenesis by inhibiting viral reactivation. PLoS Pathog. 2020;16(7):e1008701.
25. Elssner A, Doseff AI, Duncan M, Kotur M, Wewers MD. IL-16 is constitutively present in peripheral blood monocytes and spontaneously released during apoptosis. J Immunol. 2004;172(12):7721-7725.
26. Wu DM, Zhang Y, Parada NA, et al. Processing and release of IL-16 from CD4+ but not CD8+ T cells is activation dependent. J Immunol. 1999;162(3):1287-1293.
27. Bozorgmehr N, Okoye I, Oyegbami O, et al. Expanded antigen-experienced CD160(+)CD8(+)effector T cells exhibit impaired effector functions in chronic lymphocytic leukemia. J Immunother Cancer. 2021;9(4):e002189.
28. Atanackovic D, Hildebrandt Y, Templin J, et al. Role of interleukin 16 in multiple myeloma. J Natl Cancer Inst. 2012;104(13):1005-1020.
29. Basso K, Saito M, Sumazin P, et al. Integrated biochemical and computational approach identifies BCL6 direct target genes controlling multiple pathways in normal germinal center B cells. Blood. 2010;115(5):975-984.
30. Venturutti L, Melnick AM. The dangers of deja vu: memory B cells as the cells of origin of ABC-DLBCLs. Blood. 2020;136(20):2263-2274.
31. Schmitz R, Wright GW, Huang DW, et al. Genetics and pathogenesis of diffuse large B-cell lymphoma. N Engl J Med. 2018;378(15):1396-1407.
32. Chapuy B, Stewart C, Dunford AJ, et al. Molecular subtypes of diffuse large B cell lymphoma are associated with distinct pathogenic mechanisms and outcomes. Nat Med. 2018;24(5):679-690.
33. Ennishi D, Healy S, Bashashati A, et al. TMEM30A loss-of-function mutations drive lymphomagenesis and confer therapeutically exploitable vulnerability in B-cell lymphoma. Nat Med. 2020;26(4):577-588.
34. Pinney JJ, Rivera-Escalera F, Chu CC, et al. Macrophage hypophagia as a mechanism of innate immune exhaustion in mAb-induced cell clearance. Blood. 2020;136(18):2065-2079.
35. Yu J, Li S, Chen D, et al. IMM0306, a fusion protein of CD20 mAb with the CD47 binding domain of SIRPalpha, exerts excellent cancer killing efficacy by activating both macrophages and NK cells via blockade of CD47-SIRPalpha interaction and FcγR engagement by simultaneously binding to CD47 and CD20 of B cells. Leukemia. 2023;37(3):695-698.
36. Basso K, Dalla-Favera R. Germinal centres and B cell lymphomagenesis. Nat Rev Immunol. 2015;15(3):172-184.
37. Holmes AB, Corinaldesi C, Shen Q, et al. Single-cell analysis of germinal-center B cells informs on lymphoma cell of origin and outcome. J Exp Med. 2020;217(10):e20200483.
38. Venturutti L, Teater M, Zhai A, et al. TBL1XR1 mutations drive extranodal lymphoma by inducing a pro-tumorigenic memory fate. Cell. 2020;182(2):297-316.e27.
39. Cottereau AS, Meignan M, Nioche C, et al. Risk stratification in diffuse large B-cell lymphoma using lesion dissemination and metabolic tumor burden calculated from baseline PET/CT†. Ann Oncol. 2021;32(3):404-411.
40. Rivas-Delgado A, Nadeu F, Enjuanes A, et al. Mutational landscape and tumor burden assessed by cell-free DNA in diffuse large B-cell lymphoma in a population-based study. Clin Cancer Res. 2021;27(2):513-521.
41. Cubillos-Ruiz JR, Bettigole SE, Glimcher LH. Tumorigenic and immunosuppressive effects of endoplasmic reticulum stress in cancer. Cell. 2017;168(4):692-706.
42. Mulder K, Patel AA, Kong WT, et al. Cross-tissue single-cell landscape of human monocytes and macrophages in health and disease. Immunity. 2021;54(8):1883-1900.e5.
43. Steen CB, Luca BA, Esfahani MS, et al. The landscape of tumor cell states and ecosystems in diffuse large B cell lymphoma. Cancer Cell. 2021;39(10):1422-1437.e10.
44. Cassetta L, Pollard JW. Targeting macrophages: therapeutic approaches in cancer. Nat Rev Drug Discov. 2018;17(12):887-904.
45. Advani R, Flinn I, Popplewell L, et al. CD47 Blockade by Hu5F9-G4 and rituximab in non-Hodgkin's lymphoma. N Engl J Med. 2018;379(18):1711-1721.
46. Chao MP, Alizadeh AA, Tang C, et al. Anti-CD47 antibody synergizes with rituximab to promote phagocytosis and eradicate non-Hodgkin lymphoma. Cell. 2010;142(5):699-713.